OXFORD UNIVERSITY PRESS Toxicological Sciences

Arsenic increases Pi-mediated vascular calcification and induces premature senescence in vascular smooth muscle cells

Journal:	*Toxicological Sciences*
Manuscript ID:	TOXSCI-12-0715.R1
Manuscript Type:	Research Article
Date Submitted by the Author:	n/a
Complete List of Authors:	Martin-Pardillos, Ana; University of Zaragoza, Toxicology Sosa, Cecilia; University of Zaragoza, Toxicology Sorribas, Victor; University of Zaragoza, Toxicology
Key Words:	metals < Agents, cardiovascular system < Systems Toxicology, mechanisms < Systems Toxicology, cytotoxicity < In Vitro and Altenatives
Society of Toxicology Specialty Section Subject Area:	Cardiovascular Toxicology [106]

Arsenic increases Pi-mediated vascular calcification and induces premature senescence in vascular smooth muscle cells.

Ana MARTÍN-PARDILLOS, Cecilia SOSA, Victor SORRIBAS*

Department of Toxicology, University of Zaragoza, Spain

*Corresponding author: Dept. of Toxicology, Veterinary Faculty, University of Zaragoza. Calle Miguel Servet, 177. E50013 Zaragoza (Spain). E-mail: sorribas@unizar.es; phone: +34976761631; fax: +34976761612.

Running title: Vasculotoxicity and calcification of arsenic

Abstract

Several mechanisms have been proposed to explain the vascular toxicity of arsenic. Some of them are described in this work, such as stress-induced premature senescence (SIPS), dedifferentiation, and medial vascular calcification, and they all affect vascular smooth muscle cells (VSMC). Rat aortic VSMC were treated with 1-100 μM of either sodium arsenate (As^{V}), arsenite (As^{III}), monomethylarsonic acid (MMA), or dimethylarsinic acid (DMA). None of the treatments induced VSMC calcification in the presence of 1 mM inorganic phosphate (Pi), but 1 μM As^{III} did increase calcification when induced with 2.5 mM Pi. An LDH assay revealed that this increase was explained by a rise in cytotoxicity due to simultaneous incubation with 1 μM As^{III} and 2.5 mM Pi. This calcification increase was also observed in the aortas of a vascular calcification model: 5/6 nephrectomized rats fed with a high Pi diet and treated with vitamin D_3. Several known mechanisms that might explain arsenic toxicity in our experimental model were discarded: apoptosis, oxidative stress, and inflammasome activation. Nevertheless, both senescence-associated ß-galactosidase (SA ß-gal) activity and p21 expression were increased by As^{III}, which reveals the induction of SIPS. As^{III} also caused dedifferentiation of VSMC, as shown by the reduced expression of the VSMC markers SM22α and calponin. Senescence and gene expression were also observed in the aortas of healthy rats treated with 50 ppm As^{V} in drinking water for one month. In conclusion, both premature senescence in aortic VSMC with phenotypic dedifferentiation and the increase of Pi-induced calcification are novel mechanisms of arsenic vasculotoxicity.

Keywords: Arsenic, vasculotoxicity, premature senescence, vascular calcification, dedifferentiation.

Introduction

Arsenic is a ubiquitous metalloid found in the Earth's crust and is a common natural contaminant of groundwater worldwide as a result of its release from pyrite complexes. The consumption of contaminated drinking water is the most common source of chronic exposure to arsenic (e.g., Sams II et al., 2007), with adverse consequences of major proportions in some poor areas (Bhattacharjee, 2007).

The WHO has recommended a maximum concentration of 10 µg/l of inorganic As in drinking water. When this limit is exceeded, a plethora of toxic effects can appear, including cardiovascular complications and peripheral vascular disorders (for excellent reviews, see Balakumar and Kaur, 2009, and States et al., 2009).

Some of the described mechanisms of arsenic vascular toxicity include the inhibition of nitric oxide production through the blockage of eNOS, thereby impairing the vasodilatation function of endothelial cells (Kumagai and Pi, 2004). Inorganic arsenite (As^{III}) also increases the production of reactive oxygen species (ROS) after the activation of NADPH oxidase, and this increase indirectly enhances endothelial permeability by inducing the expression of vascular endothelial growth factor (VEGF) (Bao and Shi, 2010). Arsenic furthermore exacerbates atherosclerotic lesions by increasing the proliferation of vascular smooth muscle cells (VSMC), generating oxidative stress, and increasing the expression of growth factors (TGF-α), proinflammatory cytokines (TNF-α, IL-6, IL-8), monocyte chemoattractant protein-1, etc. (for reviews of this extensive subject, see Balakumar and Kaur, 2009, and Simeonova

and Luster, 2004). Hypertension and vasoconstriction are other indicators of arsenic exposure, and several species and metabolites have been shown to induce these conditions (Lee et al., 2005; Park et al., 2005; Lim et al., 2011). VSMC apoptosis has also been implicated in the vasculotoxicity of arsenic trioxide, with a concomitant increase of ROS and intracellular calcium, *in vitro* (Li et al., 2010). Similarly, the unfolded protein response, which is known as endoplasmic reticulum stress, has also been reported in several cell types exposed to arsenic (Yen et al., 2012), and this phenomenon has also been observed in other vascular disorders (Duan et al., 2009).

In brief, the various mechanisms that have been observed during arsenic vasculotoxicity include apoptosis, oxidative stress, inflammatory mediators, endoplasmic reticulum stress, etc. These phenomena have also been observed in relevant degenerative vascular disorders, such as medial vascular calcification (i.e., Monckeberg's sclerosis), a process that has been systematically observed during chronic kidney disease, diabetes, and aging (e.g., Ketteler et al., 2011).

The purpose of this work has been to test whether As could have a role in the pathogenesis of medial vascular calcification, either as an initiator or as a complicating factor. We have assayed several arsenic species and have analyzed the occurrence of the aforementioned mechanisms in rat aortic VSMC, *in vitro* and *in vivo*. Specifically, in this paper we report that As enhances and worsens the calcification of cells obtained under the hyperphosphatemic conditions observed during chronic kidney disease. We also present a novel mechanism of arsenic vascular toxicity, namely stress-induced premature senescence (Goligorsky et al., 2009), the consequences of which, while not sufficient to induce calcification, can harm the physiological integrity of the arterial wall.

Materials and Methods

***Vascular smooth muscle cells*.** Cells were obtained from the thoracic aortas of 2-month-old male Wistar rats by mechanical and collagenase digestion, as previously described (Wang et al., 2007). As explained in this same reference, the cells were maintained in Minimal Essential Medium (Gibco-Life Technologies, Paisley, UK). When the cells were confluent, they were trypsinized, counted, and passaged up to 20 divisions. The cells from the 20^{th} to the 30^{th} divisions were used. For treatments, the cells were made quiescent by reducing the concentration of fetal calf serum to 0.2%.

***In vitro* assays.** All chemicals for the arsenic assays were obtained from Sigma-Aldrich (St. Louis, MO) and were analytical grade. The incubation times and the concentrations of the chemicals are indicated in the Results section. Cell death was evaluated two ways. Colorimetrical quantitation was determined using a Cytotoxicity Detection kit (Roche, Mannheim, Germany) according to the activity of the cytosolic lactate dehydrogenase (LDH) released into the cell culture. Cell death was also evaluated by fluorescent microscopy analysis and staining of the cells with a double dye containing acridine orange and ethidium bromide (AO/EB), as described (McGahon et al., 1995). Live cells stained green with acridine orange, and only dead cells allowed ethidium bromide to enter and then fluoresced red.

Stress-induced premature senescence (SIPS) was evaluated in the same cells by determining the activity of senescence-associated ß-galactosidase (SA ß-gal) at pH 4 and 6, as described (Dimri et al., 1995), after fixing the cells with paraformaldehyde. The presence of apoptosis was determined by a terminal deoxynucleotidyl transferase

dUTP nick end labeling (TUNEL) fluorescent assay, using a Click-iT TUNEL Alexa Fluor-488 kit (Molecular Probes-Life Technologies, Paisley, UK). The cells were visualized using an Axiovert 200M fluorescent microscope (Carl Zeiss, Jena, Germany).

Several assays were performed to determine activation of the multiprotein oligomer, inflammasome: the quantification of interleukin-1ß (IL-1ß) released into the cell culture medium using an IL-1ß Rat ELISA kit (Novex-Life Technologies, Carlsbad, CA, USA), the abundance of IL-1ß transcripts by real-time PCR, and the abundance of caspase-1 by immunoblotting using a cell lysate in RIPA buffer (25 mM Tris-HCl pH 7.6, 150 mM NaCl, 1% Nonidet P-40, 1% sodium deoxycholate, and 0.1% sodium dodecyl sulfate) and a polyclonal antibody (Santa Cruz, Heidelberg, Germany). The rationale for the assays has been described elsewhere (Stienstra et al., 2011).

Three approaches were used for evaluating oxidative stress. First, the direct oxidation of proteins was determined according to the carbonyl content using an OxyELISA™ Oxidized Protein Quantitation Kit (Merck Millipore, Darmstadt, Germany). To confirm the oxidative stress status, the relative abundance of phospho-p38 was also quantified by immunoblotting using a polyclonal antibody (Sigma-Aldrich, St. Louis, MO, USA). Finally, the generation of reactive oxygen species was evaluated using a fluorescent CellROX Green Reagent (Molecular probes), which binds to DNA upon oxidation, thereby turning the nuclei and mitochondria green.

***Animal treatments*.** For *in vivo* experiments, the use of animals was conducted in accordance with the Guiding Principles on the Use of Animals in Toxicology, of the Society of Toxicology, and it was approved by the Ethical Committee of the University of

Zaragoza (code PI07/09). Two-month-old male Wistar rats were treated with 50 ppm sodium arsenate in drinking water. This water was previously checked for undetectable arsenic content. For experiments to induce vascular calcification *in vivo*, 5/6 nephrectomized (5/6 Nx) rats were purchased from Janvier SAS (Berthevin, France). Some rats were treated with 50 ppm As^V in drinking water for 30 days and were simultaneously fed fodder containing 1.2% Pi. To accelerate calcification, the animals were also intraperitoneally dosed with 80 ng/kg body weight of vitamin D_3 every two days (see the Results section for details). Fractional excretion of Pi (FE_{Pi}) was calculated as explained (Alcalde et al., 1999) using the formula $(U_{Pi}/S_{Pi})x100/(U_{Cr}/S_{Cr})$, where U is urine, S is serum, and Cr is creatinine.

***Calcification assays*.** To induce the calcification of VSMC, the cells were grown in 24-well plates and calcified as described (Villa-Bellosta and Sorribas, 2009) by incubating them in MEM with 0.2% FCS and a final concentration of 2.5 mM Pi from a stock of KH_2PO_4 and K_2HPO_4, pH 7.4. Alizarin red staining was used to qualitatively visualize the calcification of VSMC *in vitro* as described (Villa-Bellosta and Sorribas, 2009). For the microscopic analysis of aorta calcification, we used both Alizarin red and von Kossa staining of tissue slides, as reported (Verberckmoes et al., 2007). For the quantitative determination of calcium content, VSMC cultures or rat aortas were incubated overnight in 0.6 N HCl, and the dissolved calcium was quantified using a colorimetric Calcium Assay kit (Abnova, Taipei, Taiwan).

Microscopy analysis. VSMC were grown in culture slides (BD Falcon, Erembodegem, Belgium), and after the corresponding treatments the cells were fixed using 4% paraformaldehyde in PBS and processed as described (Lanaspa et al., 2007) for

fluorescence analysis using an Axiovert 200M microscope equipped with ApoTome for structured illumination and colocalization. For tissue sections, aortas were stripped by microscopic dissection and fixed by immersion in two steps: first, 15 min. at 4º C in 1.5% paraformaldehyde / 0.1% glutaraldehyde in PBS, then 2 hours at 4º C in 1.5% paraformaldehyde / 0.1% glutaraldehyde / 20% sucrose in PBS. The aortas were then cryoprotected in 20% sucrose for 1 hour at 4º C, mounted in OCT, and frozen. Cryosections were cut at 6 µM and -30º C in a Leica CM1850 cryostat (Wetzlar, Germany). After neutralization with glycine, the slides were blocked with 10% BSA and 1% Tween-20 in PBS for 20 min., and then they were incubated overnight with the primary antibody in 10% BSA and 1% Tween-20 in PBS. After washing, the secondary antibody was dissolved in the same solution and incubated for 30 minutes at room temperature. The slides were then mounted using Prolong antifade reagent with DAPI (Molecular Probes).

***Immunoblotting*.** The protein from cell lysates in RIPA buffer was quantified using a BCA Protein Assay kit (Pierce, Rockford, IL, USA). Immunoblotting was performed as described (Villa-Bellosta et al., 2009), with instrumental modifications, including the use of a Trans-Blot Turbo Transfer System for PVDF membranes and detection using a Molecular Imager VersaDoc MP 4000 System (both from Bio-Rad, Hercules, CA, USA).

Real-time PCR. Total RNA was purified from cultured VSMC using a GenElute Mammalian Total RNA Miniprep Kit. After DNAse I treatment, the RNA was retrotranscribed and amplified in a LightCycler 1.5 using a LightCycler FastStart Master SYBR Green I kit (all from Roche, Mannheim, Germany). For relative quantification, acidic ribosomal phosphoprotein (Arp) RNA was used as an endogenous reference, and

a calibrator was included according to the manufacturer's instructions, as previously described (Villa-Bellosta et al., 2011).

Data analysis. Each type of experiment was repeated at least twice, with similar results. Regarding the determination of LDH activity and the quantitation of deposited calcium, the experiments were performed three times to obtain more accurate results. In all the experiments, three determinations were obtained for each condition. The data were statistically analyzed using GraphPad Prism 5.0 for Mac (GraphPad Software Inc., La Jolla, CA, USA). The significances of differences were determined by a one-way analysis of variance (ANOVA) and a Tukey post-test for multiple comparisons.

Results

Cytotoxicity of arsenic species

The cytotoxicities of sodium arsenate (As^{V}) and sodium arsenite (As^{III}) and of the two methylated metabolites, monomethylarsonic acid (MMA) and dimethylarsinic acid (DMA), in rat aortic VSMC grown in culture were assayed using an LDH kit. Several concentrations and incubation times were tested, as shown in Figures 1A through D. Toxicity was significant after 1 day at 100 µM As^{III} and after 5 days at 10 µM. As^{V} toxicity was only evident after 3 days at 100 µM. DMA and MMA were not cytotoxic even after 5 days and at 100 µM each. On the other hand, LDH activity was not modified by any of the arsenicals or concentrations used, given that none of the arsenicals at any concentration diminished the activity obtained with the positive control, i.e., 2% Triton X-100 for one hour (data not shown).

These findings were also obtained using a microscopic method: the double staining with acridine orange / ethidium bromide (Fig. 1E). After 5 days of incubation with 10 µM As^{III}, the percentage of red cells increased to a level that was similar to the one obtained using the LDH method. These data led us to choose non-cytotoxic concentrations for the following studies.

Effect of arsenic on calcification "in vitro"

To determine if As could induce calcification under either control or basal conditions, VSMC were incubated with increasing but non-cytotoxic concentrations of As^{III} for 5 days (Fig. 2). Under these normophosphatemic concentrations, i.e., in the presence of 1

mM Pi, As^{III} did not induce calcification of the cells, as shown by the absence of staining with Alizarin red and by the quantity of calcium content (Figures 2A and B). However, As^{III} did increase the calcification of cells incubated under calcifying conditions, i.e., in the presence of 2.5 mM Pi (equivalent to hyperphosphatemic concentrations; e.g., Jono et al., 2000), as observed during chronic renal failure.

To differentiate whether the effect of arsenic on calcification was mediated by a biological mechanism in the cells or by a physical mechanism acting either on the initiation or on the rate of calcium phosphate deposition, we used our model of passive calcification (Villa-Bellosta and Sorribas, 2009). Consequently, not only was the effect of As assayed again in live cells, as before, it was also assayed in dead cells that were previously killed by fixation with 4% paraformaldehyde. As expected, the intensity of calcification was greater in dead cells than in live cells, under any condition (Fig. 2C). However, the increasing effect of arsenic on calcification was only observed in live cells. This dependence on live cells eliminated the possibility of a single physical effect by arsenic, e.g., by increasing the rate of nucleation.

Even though we determined that As^{III} was not cytotoxic at the given concentrations (Fig. 1A), we also checked whether the combination of As^{III} and a high concentration of Pi could increase VSMC death, given that cell death is a well-known cause of calcification. Fig. 2D shows the different combinations of Pi and As^{III} concentrations and the LDH response as a measure of cell death. It can be seen that the combination of 2.5 mM Pi and 1 μM As^{III} increased the death of VSMC, and this increase is therefore the likely cause of the higher calcification observed under the hyperphosphatemic concentrations observed in the presence of arsenic.

Arsenic increases calcification "in vivo"

To confirm that the increase in calcification was not an artifact of the *in vitro* model and that it also occurs *in vivo*, we used the 5/6 nephrectomized (Nx) rat model of chronic kidney disease and vascular calcification (Shobeiri *et al*., 2010). Three groups of rats were used: control (non-Nx), Nx, and Nx+As. The animals were induced to calcify using a 1.2% Pi diet and a vitamin D_3 dosage (80 ng/kg) to accelerate calcification. In addition, the Nx+As rats were 5/6 Nx treated with 50 ppm As^V in the drinking water. As^{III} was not used, because it is much more toxic than As^V and because As^V is reduced to As^{III} in blood and tissues. After one month of treatment, the animals were anesthetized by injection with thiopental, and both the hearts and aortas were dissected and processed for calcium content and histology. Table 1 shows the growth and the food and water consumption of the animals, the parameters of chronic kidney disease, and the arsenic concentration in plasma. All 5/6 Nx rats showed reduced growth rates and even weight loss after administering calcitriol, accompanied by reduced food consumption, elevated urea and creatinine concentrations, and an increased fractional excretion of Pi. The aortas of the control group were normal, smooth and flat, while the aortas of the Nx and Nx+As groups were twisted and folded, a finding compatible with advanced sclerosis due to medial calcification of the aorta (Fig. 3A). The calcium content in the complete rat aortas of the Nx group was 76% higher than the content in the control animals, and this percentage further increased to 187% in the Nx+As group. Figure 3B shows the calcium content of the thoracic and abdominal aortas separately, where similar increases can be observed in both cases.

When histological sections of the aortas were stained for calcium content (Alizarin red), we observed increases that were similar to the quantitative determinations. There were clear, positive deposits in the Nx animals, which deposits were more extensive in the Nx+As animals (Fig. 3C). Similar findings were observed when we stained for phosphate content (von Kossa, Fig. 3C). In the absence of 5/6-Nx (control), no calcification was observed, even with the simultaneous treatment of 1.2% Pi and calcitriol.

Excluded mechanisms of arsenic toxicity "*in vitro*"

In addition to the increase in vascular calcification caused by arsenic, we also tested alternative mechanisms of toxicity in VSMC. First, the induction of apoptosis was determined by a fluorescent TUNEL assay on VSMC incubated for 5 days in the presence of 5 and 10 μM As^{III} or 10 μM As^{V}. Fig. 4A shows no evidence of apoptosis under these conditions and using this methodological approach.

Another reported vasculotoxic mechanism of As pertains to oxidative stress. To measure the extent of this insult, we quantified the following: the production of reactive oxidative species using a CellROX green reagent, the accumulation of carbonyl groups in proteins, and the expression of the phosphorylated stress protein p38 (Figures 4A, B, and C, respectively). VSMC were treated as above for the apoptosis assay. Regarding the CellROX, cells were incubated with the reagent for 30 minutes and then fixed with 3.7% paraformaldehyde, as suggested by the manufacturer. In no case did we find any significant increase in the oxidative parameters. On the contrary, it was surprising to observe that, regarding the determination of carbonyl content and the quantitation of

phospho-p38 abundance, arsenic seemed to reduce the signs of oxidative damage, and in the case of phospho-p38 the difference became statistically significant.

Finally, the activation of inflammasome was also tested according to the expression of Il-1ß in culture medium (Fig. 4E), the quantification of the corresponding RNA transcript (data not shown), and the expression of the different forms of caspase-1 (Fig. 4F). Again, no changes were observed in the expression of IL-1ß protein and RNA, or in the abundance of pro- and mature caspase-1, after exposure to As^{III} or As^{V} for 3 and 5 days. Therefore, the activation of inflammasome was discarded as a mechanism of arsenic toxicity.

Stress-induced premature senescence of VSMC "in vitro" and "in vivo"

This newly reported mechanism of toxicity was also tested for arsenic in rat VSMC. The cells were incubated with 1 and 10 μM of either As^{III} or As^{V} for 5 days, and then they were assayed for the activity of (SA ß-gal) galactosidase at pH 4 and 6. Fig. 5A shows that the activity of this lysosomal enzyme was already increasing at 1 μM As^{III}, and it was maximal at 10 μM. Similarly to MMA and DMA, As^{V} did not have any effect on ß-Gal (data not shown). An increase in SA ß-Gal activity was prevented by simultaneous incubation with 10 μM of resveratrol (RV).

The increased activity of SA ß-Gal was not due to cell aging, rather it was due to this specialized form of cell senescence, given that there was no change in the abundance of the nuclear protein lamin A/C (Fig. 5B). The effect of As on SIPS was confirmed by determining the abundance of the p21 marker. The expression of p21 was maximally increased by treating with As^{III} and was only minimally increased by As^{V}, although the

difference was not statistically significant for As^{V} (Fig. 5C). In this case, resveratrol (10 μM) did not prevent the increase of p21 expression, rather it actually seemed to increase expression in the presence of 0 and 5 μM As^{III}, although the apparent effect was once again not statistically significant (Fig. 5D).

Given that resveratrol prevented the induction of SIPS by As^{III}, we also tested whether resveratrol could prevent the calcification induced by As^{III} and a high Pi medium. Fig. 5E shows that resveratrol did not prevent calcification induced either by 2.5 mM Pi or the additional increase of calcification caused by As^{III}. The absence of an effect by resveratrol on calcification suggests that SIPS is not related to calcification. Nevertheless, to clarify this point we designed an experiment to differentiate between the effect of As on SIPS induction and the effect of arsenic on additional calcification induction. First, to induce senescence we incubated VSMC for 5 days with As^{III} at the concentrations indicated in Fig. 5F, in the presence of a normal culture medium (i.e., 1 mM Pi). We then changed the medium and incubated the cells using a calcifying medium (2.5 mM Pi) without As^{III} for an additional 5 days. In this case, no further increase in calcification was observed, wherefore the mechanism of SIPS induction can be ruled out as the basis for the effect by As on calcification.

Finally, to check that the induction of SIPS by As was not simply related to our vascular cell model but that it also happened *in vivo*, we treated male Wistar rats for one month with drinking water that contained 50 ppm arsenate. Whole aortas were processed for SA ß-gal activity, and the results are shown in Fig 6A. Arsenate clearly increased the lysosomal ß-gal activity, which confirms the existence of this vasculotoxic mechanism of arsenic *in vivo*. We also measured the calcium content of these aortas, and as

expected, no change due to treatment with arsenic was observed (Fig. 6B). The expression of both p21 and lamin A/C was also determined by fluorescent immunohistochemistry in these animals, and the results of our *in vitro* data were confirmed, i.e., no effect on lamin A/C expression and increased p21 abundance (Fig. 6C).

Arsenic induces dedifferentiation of VSMC

The origin of VSMC is mesenchymal, and VSMC can easily *trans*-differentiate *in vitro* and *in vivo* under several circumstances, including calcification conditions (see the Discussion section). Therefore, by determining the expression of VSMC markers after incubation for 5 days with As^{III} at 5 and 10 µM or with As^{V} at 10 µM, we checked if arsenic could modify the pattern of gene expression that is characteristic of vascular smooth muscle cells. The expressions of α-actin and SM22α were determined by immunoblotting (Fig. 7A), which showed a reduction of approximately 40% in SM22α expression in both oxidative states of the metalloid at 10 µM. α-Actin and α-tubulin were not modified. The change in SM22α expression was confirmed by real-time PCR (Fig. 7B), and the analysis was extended to calponin and to the matrix Gla protein (we did not have reliable antibodies for immunoblotting). In these two cases, the inhibitory effect of arsenite was very strong, showing dramatic inhibitions of 89% and 97% in the expressions of calponin and MGP, respectively, compared to the control condition. With respect to arsenate, inhibition was more moderate regarding SM22α, and calponin and MGP RNAs showed inhibitions of 43% and 60%, respectively.

The results for α-actin, SM22α, and calponin in As^{III}-treated VSMC were confirmed by fluorescent immunocytochemistry, showing findings similar to those for immunoblotting and real-time PCR (Fig. 8). In rat, the reductions in the expression of both SM22α and calponin, as well as the absence of an effect on α-actin, were confirmed by fluorescent immunohistochemistry in the aortas of rats treated for one month with 50 ppm As^{V} in drinking water (Fig. 6C).

Discussion

Metalloid arsenic is one of the few natural xenobiotics that still significantly threaten human beings and domestic animals, mainly through chronic consumption of contaminated water. The vascular system seems to be a key target among the many toxic effects caused by arsenic exposure, and it is affected through several mechanisms, some of which have been mentioned in the Introduction and are well described in literature (e.g., Balakumar and Kau, 2009; States et al., 2009). In this work we have studied several aspects related to vascular exposure to arsenic, and we have found significant events related to cytotoxicity/senescence and the dedifferentiation of vascular smooth muscle cells that are common to the pathogenesis of medial vascular calcification. Therefore, we initially focused on the possibility that arsenic could participate in the development of this vascular disorder (Monckeberg's sclerosis), and we concluded that arsenic is not sufficient to induce the calcification of vascular smooth muscle cells *in vitro* under physiological concentrations of Pi and Ca and at the moderated concentrations of As that were used (Fig. 2). However, arsenic does increase experimental calcification induced with 2.5 mM Pi (a concentration frequently reached during CKD-derived hyperphosphatemia), namely it worsens the calcification level of VSMC obtained under calcifying conditions. This effect most likely occurs through a cytotoxic mechanism, because cell death is increased by the simultaneous presence of arsenic and a high concentration of Pi, and cell death is a well-documented cause of calcium phosphate deposition (see Reynolds et al., 2004). Our findings are not simply an artifact of the *in vitro* model and of the particular experimental conditions; on the contrary, we have reproduced the phenomenon in rats using an *in vivo* model of

chronic kidney disease with calcification (Fig. 3). The detrimental effect of arsenic occurred similarly in both anatomical parts of the aorta, namely the thoracic and abdominal sections. The Nx animals showed hyperphosphatemia and high fractional excretion of Pi (FE_{Pi}) as a consequence of the high Pi intake and, most likely, the increased phosphatonin FGF23 plasma levels (the calcium concentration did not change in the plasma, because the animals were calcitriol-treated, and therefore the parathyroid hormone should also exhibit normal plasma levels with no effect on FE_{Pi}). The additional effect by As on Pi-induced calcification in nephrectomized animals is an important pathological finding, which is likely to have repercussions for chronic kidney disease patients living in areas of high arsenic exposure. This finding is relevant despite the high dose of arsenic and the extreme calcifying conditions used to obtain results within a reasonable frame time. While these conditions need to be fine-tuned and refined in future works, for now they do corroborate the *in vitro* findings and represent a new research alert in the field of arsenic exposure during chronic kidney disease, in which the interaction between arsenic and inorganic phosphate deserves further attention.

As regards other mechanisms of arsenic toxicity that have been described in other works, such as apoptosis accumulation, oxidative stress, or inflammasome activation, we have not found evidence of these mechanisms in this work (Fig. 4), most likely because the experimental conditions or the cell model were different. However, we have observed two new phenomena in VSMC exposed to arsenic, which seem to be unrelated to vascular calcification. First, arsenic induces the premature senescence of VSMC, which is a toxic response obtained with stressors acting at lower concentrations

or intensities than those usually required for apoptosis or cell necrosis and which is responsible for a significant functional deficit of vessels (for a review, see Chen et al., 2008). A similar effect by arsenic as a SIPS inducer in mesenchymal stem cells has recently been described (Cheng et al., 2011). SIPS cells actively metabolize, but with the cell cycle arrested, and they show impaired functionality. SIPS cells are distinguished from replicative senescent cells (i.e., cells that are near the Hayflick limit and that accumulate with age) by the fact that only the latter suffer from telomerase activity reduction and genomic instability derived from telomere attrition (Goligorsky et al., 2009). Other hallmarks of cell senescence, such as increased lysosome permeability (and therefore increased ß-galactosidase activity) or the overexpression of p53, p21, and p16, are present in both types of senescent cells. In our study, we determined the presence of arsenic-induced SIPS cells *in vitro* (Fig. 5) and *in vivo* (Fig. 6). Under both experimental conditions we also observed increased SA ß-gal activity and p21 expression but no changes in nuclear instability, such as lamin A/C accumulation (Ragnauth et al., 2010), which concurs with the absence of shortened telomere length.

The accumulation of senescent cells in tissues as a consequence of either aging or cellular stress can explain the functional decline of the affected tissues (Lähteenvuo and Rosenzweig, 2012). This decline can be related to a second phenomenon that we have observed in VSMC exposed to arsenic, namely dedifferentiation of the cells. The origin of VSMC is mesenchymal, and they show the ability to trans-differentiate by expressing genes that are usually silenced in this cell type (Iyemere et al., 2006; Majesky, 2007). For example, during the ectopic calcification observed in chronic kidney disease, the

expression of several osteogenes in VSMC has been described, either as the cause of calcification (Moe and Chen, 2004) or as an attempt by cells to organize the deposits of calcium phosphates (Villa-Bellosta et al., 2011). As regards arsenic, while we did not observed any calcification of VSMC unless critical changes in the concentrations of Pi (or calcium) were reached (Figures 2 and 3), exposure to arsenic did modify the expression of genes that are characteristic of or even specific to differentiated VSMC, such as SM22α or calponin (Figures 7 and 8). We do not have a feasible explanation for the absence of any observed effects on α-actin expression, other than the experimental conditions (incubation times and the concentrations of the reagents used). Nevertheless, it is evident that the loss of the full differentiation of VSMC can have dramatic consequences for the proper functioning of the vascular wall.

In summary, in addition to the multitude of described detrimental effects by arsenic on the vascular system, we can now include the accumulation of premature senescent smooth muscle cells with a dedifferentiated phenotype in the vascular wall, which can contribute to the malfunctioning of the contractile activity of the arterial wall. An increase in cytotoxicity and calcification under hyperphosphatemic conditions should also be considered in patients with chronic kidney disease who are exposed to moderate concentrations of arsenic.

Funding Information

This work was supported by the Spanish Ministry of Science and Innovation [grant number BFU2009-12763/BFI to V.S.] and by a predoctoral fellowship from the Government of Aragon (Spain) [B008/09] to A.M.P.

References

Alcalde, A.I., Sarasa, M., Raldúa, D., Aramayona, J., Morales, R., Biber, J., Murer, H., Levi, M., and Sorribas, V. (1999). Role of thyroid hormone in regulation of renal phosphate transport in young and aged rats. *Endocrinology* **140,** 1544-1551.

Bao, L., and Shi, H. (2010). Arsenite induces endothelial cell permeability increase through a reactive oxygen species-vascular endothelial growth factor pathway. *Chem. Re.s Toxicol*. **23**, 1726-1734.

Balakumar P, and Kaur J. (2009). Arsenic exposure and cardiovascular disorders: an overview. *Cardiovasc. Toxicol*. **9**, 169-176.

Bhattacharjee, Y. (2007). A sluggish response to humanity's biggest mass poisoning. *Science* **315**, 1659-1661.

Chen, J., Patschan, S., and Goligorsky, M.S. (2008). Stress-induced premature senescence of endothelial cells. *J. Nephrol.* **21**, 337-344.

Cheng, H., Qiu, L., Zhang, H., Cheng, M., Li, W., Zhao, X., Liu, K., Lei, L., and Ma, J. (2011). Arsenic trioxide promotes senescence and regulates the balance of adipogenic and osteogenic differentiation in human mesenchymal stem cells. *Acta. Biochim. Biophys. Sin.* **43**, 204–209.

Dimri, G.P., Lee, X., Basile, G., Acosta, M., Scott, G., Roskelley, C., Medrano, E.E., Linskens, M., Rubelj, I., Pereira-Smith, O., Peacocke, M., and campisi, J. (1995). A biomarker that identifies senescent human cells in culture and in aging skin in vivo. *Proc. Natl. Acad. Sci. USA*. **92**, 9363-9367.

Duan, X., Zhou, Y., Teng, X., Tang, C., and Qi, Y. (2009). Endoplasmic reticulum stress-mediated apoptosis is activated in vascular calcification. *Biochem. Biophys. Res. Commun*. **387**, 694-699.

Goligorsky, M.S., Chen, J., and Patschan, S. (2009). Stress-induced premature senescence of endothelial cells: a perilous state between recovery and point of no return. *Curr. Opin. Hematol*. **16**, 215-219.

Iyemere, V.P., Proudfoot, D., Weissberg, P.L., and Shanahan, C.M. (2006). Vascular smooth muscle cell phenotypic plasticity and the regulation of vascular calcification. *J. Intern. Med.* **260,** 192-210.

Jono, S., McKee, M.D., Murry, C.E., Shioi, A., Nishizawa, Y., Mori, K., Morii, H., and Giachelli, C.M. (2000). Phosphate regulation of vascular smooth muscle cell calcification. *Circ Res*. **87,** E10-E17.

Ketteler, M., Rothe, H., Krüger, T., Biggar, P.H., Schlieper, G. (2011). Mechanisms and treatment of extraosseous calcification in chronic kidney disease. *Nat Rev Nephrol*. **7**,509-516.

Kumagai, Y., and Pi, J. (2004). Molecular basis for arsenic-induced alteration in nitric oxide production and oxidative stress: implication of endothelial dysfunction. *Toxicol. Appl. Pharmacol.* **198**, 450–457.

Lähteenvuo, J., and Rosenzweig, A. (2012). Effects of aging on angiogenesis. *Circ. Res.* **110,** 1252-1264.

Lanaspa, M.A., Giral, H., Breusegem, S.Y., Halaihel, N., Baile, G., Catalán, J., Carrodeguas, J.A., Barry, N.P., Levi, M., and Sorribas, V. (2007). Interaction of MAP17

with NHERF3/4 induces translocation of the renal Na/Pi IIa transporter to the trans-Golgi. *Am. J. Physiol. Renal. Physiol*. **292**, F230-242.

Lee, M. Y., Lee, Y. H., Lim, K. M., Chung, S. M., Bae, O. N., Kim, H., Lee, C.R., Park, J.D., and Chung, J.H. (2005). Inorganic arsenite potentiates vasoconstriction through calcium sensitization in vascular smooth muscle. *Environ. Health. Perspect.* **113**, 1330–1335.

Li, J.X., Shen, Y.Q., Cai, B.Z., Zhao, J., Bai, X., Lu, Y.J., and Li, X.Q. (2010). Arsenic trioxide induces the apoptosis in vascular smooth muscle cells via increasing intracellular calcium and ROS formation. *Mol. Biol. Rep*. **37**,1569-76.

Lim, K.M., Shin, Y.S., Kang, S., Noh, J.Y., Kim, K., Chung, S.M., Yun, Y.P., and Chung, J.H. (2011). Potentiation of vasoconstriction and pressor response by low concentration of monomethylarsonous acid (MMA(III)). *Toxicol. Lett.* **205**, 250–256.

Majesky, M.W. (2007). Developmental basis of vascular smooth muscle diversity. *Arterioscler. Thromb. Vasc. Biol.* **27,** 1248-1258.

McGahon, A.J., Martin, S.J., Bissonnette, R.P., Mahboubi, A., Shi, Y., Mogil, R.J., Nishioka, W.K., and Green, D.R. (1995). The end of the (cell) line: methods for the study of apoptosis in vitro. In Cell Death, Methods in Cell Biology (L.M. Schwartz and B.A. Orborne, Eds.), vol. 46, pp. 153–185. Academic Press, San Diego.

Moe, S.M., and Chen, N.X. (2004). Pathophysiology of vascular calcification in chronic kidney disease. *Circ. Res.* **95,** 560-567.

Park, T.-G., Seong, Y.J., Suk, K.H., Ha, J.-H., and Kim, I.K. (2005). Enhanced contractility of vascular smooth muscle after brief exposure to arsenate. *Environ. Health Perspect*. **19**, 305–311.

Ragnauth, C.D., Warren, D.T., Liu, Y., McNair, R., Tajsic, T., Figg, N., Shroff, R., Skepper, J., and Shanahan, C.M. (2010). Prelamin A acts to accelerate smooth muscle cell senescence and is a novel biomarker of human vascular aging. *Circulation* **121,** 2200-2210.

Reynolds, J.L., Joannides, A.J., Skepper, J.N., McNair, R., Schurgers, L.J., Proudfoot, D., Jahnen-Dechent, W., Weissberg, P.L., and Shanahan. C.M. (2004). Human vascular smooth muscle cells undergo vesicle-mediated calcification in response to changes in extracellular calcium and phosphate concentrations: a potential mechanism for accelerated vascular calcification in ESRD. *J. Am. Soc. Nephrol*. **15,** 2857-2867.

Sams, R. II, Wolf, D.C., Ramasamy, S., Ohanian, E., Chen, J., and Lowit, A. (2007). Workshop overview: arsenic research and risk assessment. *Toxicol. Appl. Pharmacol.* **222**, 245-251.

Shobeiri, N., Adams, M.A. and Holden, R.M. (2010). Vascular calcification in animal models of CKD: A review. *Am. J. Nephrol*. **31,** 471-481.

Simeonova, P.P., and Luster, M.I. (2004). Arsenic and atherosclerosis. *Toxicol. Appl. Pharmacol*. **198**, 444-449.

States, J.C., Srivastava, S., Chen, Y., and Barchowsky, A. (2009). Arsenic and cardiovascular disease. *Toxicol. Sci*. **107**, 312-323.

Stienstra, R., van Diepen, J.A., Tack, C.J., Zaki, M.H., van de Veerdonk, F.L., Perera, D., Neale, G.A., Hooiveld, G.J., Hijmans, A., Vroegrijk, I., van den Berg, S., Romijn, J., Rensen, P.C., Joosten, L.A., Netea, M.G., and Kanneganti, T.D. (2011). Inflammasome is a central player in the induction of obesity and insulin resistance. *Proc. Natl. Acad. Sci. USA.***108**, 15324-15329.

Verberckmoes, S.C., Persy, V., Behets, G.J., Neven, E., Hufkens, A., Zebger-Gong, H., Müller, D., Haffner, D., Querfeld, U., Bohic, S., De Broe, M.E., and D'Haese, P.C. (2007). Uremia-related vascular calcification: more than apatite deposition. *Kidney. Int*. **71**, 298-303.

Villa-Bellosta, R., Levi, M., Sorribas, V. (2009) Vascular smooth muscle cell calcification and SLC20 inorganic phosphate transporters: effects of PDGF, TNF-alpha, and Pi. *Pflugers Arch*. **458,** 1151-1161.

Villa-Bellosta R, and Sorribas V. (2009). Phosphonoformic acid prevents vascular smooth muscle cell calcification by inhibiting calcium-phosphate deposition. *Arterioscler. Thromb. Vasc. Biol.* **29**, 761-766.

Villa-Bellosta, R., Millan, A., and Sorribas, V. (2011). Role of calcium-phosphate deposition in vascular smooth muscle cell calcification. *Am. J. Physiol. Cell Physiol.* **300,** C210-C220.

Wang, C.C., Sorribas, V., Sharma, G., Levi, M., and Draznin, B. (2007). Insulin attenuates vascular smooth muscle calcification but increases vascular smooth muscle cell phosphate transport. *Atherosclerosis* **195**, e65-75.

Yen, Y.P., Tsai, K.S., Chen, Y.W., Huang, C.F., Yang, R.S., and Liu, S.H. (2012). Arsenic induces apoptosis in myoblasts through a reactive oxygen species-induced endoplasmic reticulum stress and mitochondrial dysfunction pathway. *Arch. Toxicol*. **86**, 923-933.

Figure Legends

Figure 1: Cytotoxicity of arsenic species on VSMC from rat aortas. A through D, cytotoxicity as a function of cytosolic LDH activity in culture medium. A and B, data as a function of incubation days. C and D, cytotoxicity of arsenite and arsenate as a function of concentration, at different incubation times. 100% of LDH activity refers to maximal toxicity obtained with 2% Triton-X-100 for one hour. E. Determination of cytotoxicity by fluorescence microscopy obtained with AO/EB double staining. The number of red cells (ethidium bromide staining) slightly increases significantly after 5 days of treatment with 10 µM As^{III}. Positive control: cells fixed with 100% methanol in PBS for 5 minutes.

Figure 2: Effect of As^{III} on the calcification of VSMC in the presence of normal (1 mM) or high concentrations (2.5 mM) of Pi. A. Alizarin red staining. B. Quantification of calcium using the same conditions as in A. C. Effect of As^{III} on the calcification of either live (white bars) or dead (black bars) cells in the presence of 2.5 mM Pi, showing that the dose-dependent increase in calcification is dependent on cellular activity. D. Cytotoxicity of VSMC with the indicated concentrations of Pi and As^{III}.

Figure 3: Effect of As^{V} on the calcification of aorta *in vivo,* in rats fed with a high Pi content diet (1.2% Pi), plus 80 ng/kg bw of vitamin D_3 intraperitoneally. In addition, Nx and Nx+As animals were 5/6-nephrectomized, and Nx+As animals drank water containing 50 ppm arsenate. A. Macroscopic views of three typical specimens. B. Quantification of calcium content in thoracic vs. abdominal aortas. C. Alizarin red and von Kossa stainings of thoracic aorta sections.

Figure 4. Analysis of potential mechanisms of As toxicity in VSMC. When not shown, the cells were incubated for 5 days with the indicated arsenicals. A. No detection of either apoptosis or oxidative damage. Top, apoptosis determination by a TUNEL assay; positive control: cells treated with DNAse I. Bottom, oxidative stress determination using CellROX fluorescent dye; positive control: cells treated with 1 mM H_2O_2 for 1 hour. B and C. Analysis of oxidative stress by the nmoles of carbonyl content/mg protein (B) and the abundance of phosphorylated p38 (C), respectively. D and E. Analysis of inflammasome activation by quantifying the abundance of mature IL-1ß and the forms of p45 and p10 from procaspase-1 and caspase-1, respectively. The density of the bands in C and E were normalized with respect to ß-actin, and the ratios are expressed relative to the control conditions.

Figure 5. Effect of As on premature senescence. A. SA ß-gal activity in VSMC treated with As^{III} or As^{V}, which is prevented with resveratrol treatment. B. Absence of the accumulation of the nuclear matrix protein lamin A/C. C. Induction of p21 expression with As^{III}. D. Resveratrol does not prevent the increase of p21 expression. E. Pi-induced calcification is also not prevented with 10 µM resveratrol or the additional calcification increase caused by 2.5-5 µM As^{III}. F. The senescence of VSMC was first induced with As^{III} only, and then the cells were induced to calcify with 2.5 mM Pi in the absence of As^{III}. In this case, As^{III} did not modify the calcification obtained with a high Pi concentration. The relative expression in immunoblotted signals (B to D) was calculated after normalization with respect to ß-actin intensity, and then the corresponding ratios are expressed relative to the control condition.

Figure 6. Effect of arsenic on rat aorta *in vivo*. Rats were treated for one month with 50 ppm As^{V} in drinking water and then the following determinations were obtained: A. SA ß-gal activity. B. Quantification of calcium deposits. C. Immunofluorescence images of the expression of the indicated proteins, showing an increase of p21 expression but a decrease of SM22α and calponin abundance. Blue, DAPI; red or green corresponds to the respectively indicated protein.

Figure 7. Arsenic induces dedifferentiation of VSMC after 5 days of treatment with As^{III} or As^{V}. A. Immunoblots of the relative abundance of α-actin, α-tubulin, and SM22α. B. The relative quantification of SM22α, calponin, and matrix Gla protein (MGP) RNA transcript abundances by real-time PCR. The relative expression in immunoblotted signals (A) was calculated after normalization with respect to ß-actin intensity, and then the corresponding ratios are expressed relative to the control condition.

Figure 8. Immunofluorescence imaging of VSMC treated or not treated with 10µM As^{III} to visualize α-actin, SM22α, and calponin. Blue, DAPI staining of nuclei.

Table 1. Blood plasma values of renal and calcification parameters.

Group	Urea (mg/dl)	Creatinine (mg/dl)	Ca (mg/dl)	Pi (mg/dl)	As (µg/l)	FE_{Pi} (%)	Final Weight (g)	% Growth	Water (ml/rat/day)	Food (g/rat/day)
Control	20.7 ± 1.3	0.5 ± 0.0	10.4 ± 0.2	6.7 ± 0.2	17.0 ± 9.6	25.4 ± 3.9	510 ± 10.4	88.2 ± 3.8	32 ± 0.5	26 ± 0.7
Nx	121.0 ± 33.8*	1.6 ± 0.2*	10.1 ± 0.8	10.0 ± 1.0	12.7 ± 4.7	64.0 ± 6.8*	353 ± 22.4*	3.3 ± 6.6*	38 ± 1.5*	16 ± 2.7*
Nx+As	109.0 ± 9.1*	1.6 ± 0.2*	9.6 ± 0.6	12.3 ± 2.2	2209 ± 157*	60.2 ± 1.2*	332 ± 13.6*	-1.6 ± 4.0*	23 ± 1.8*	13 ± 1.4*

Values are expressed as mean ± sem. *Significantly different with respect to the Control. Water and Food refer to consumption per animal.

Figure 1

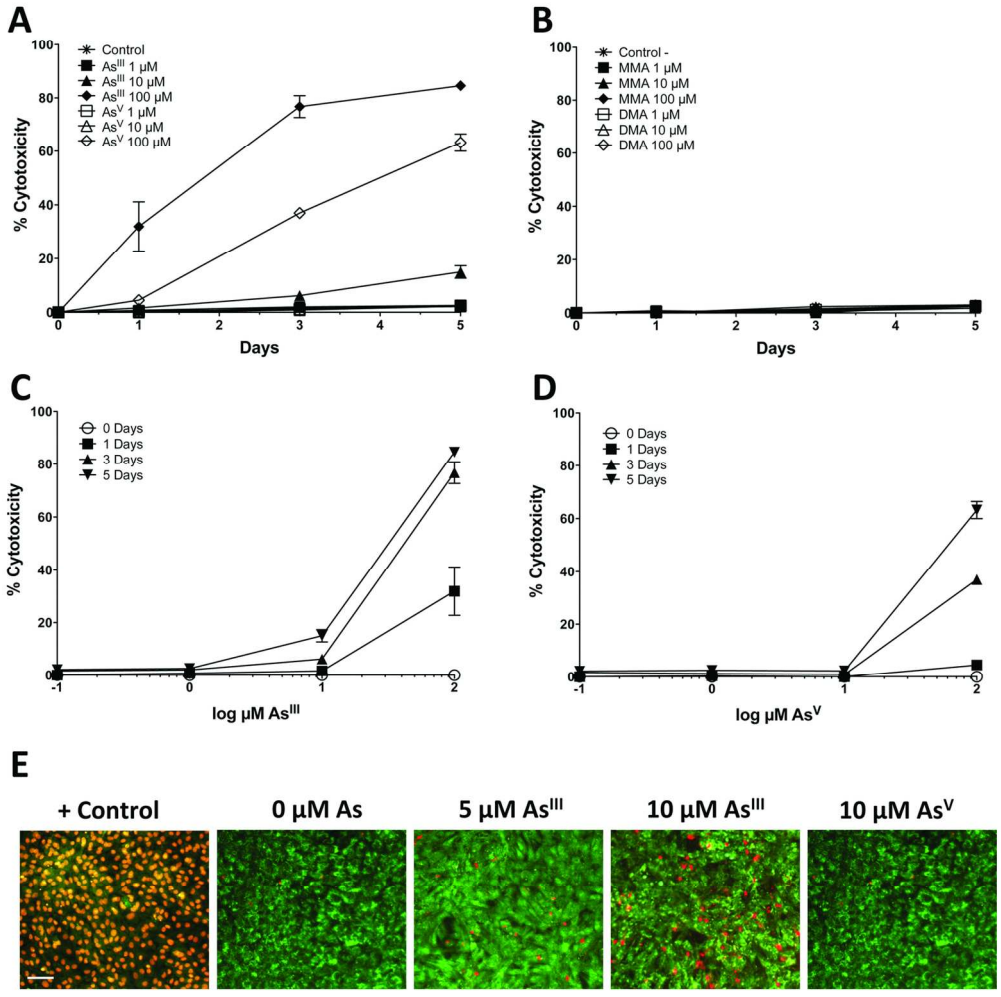

140x148mm (300 x 300 DPI)

Figure 2

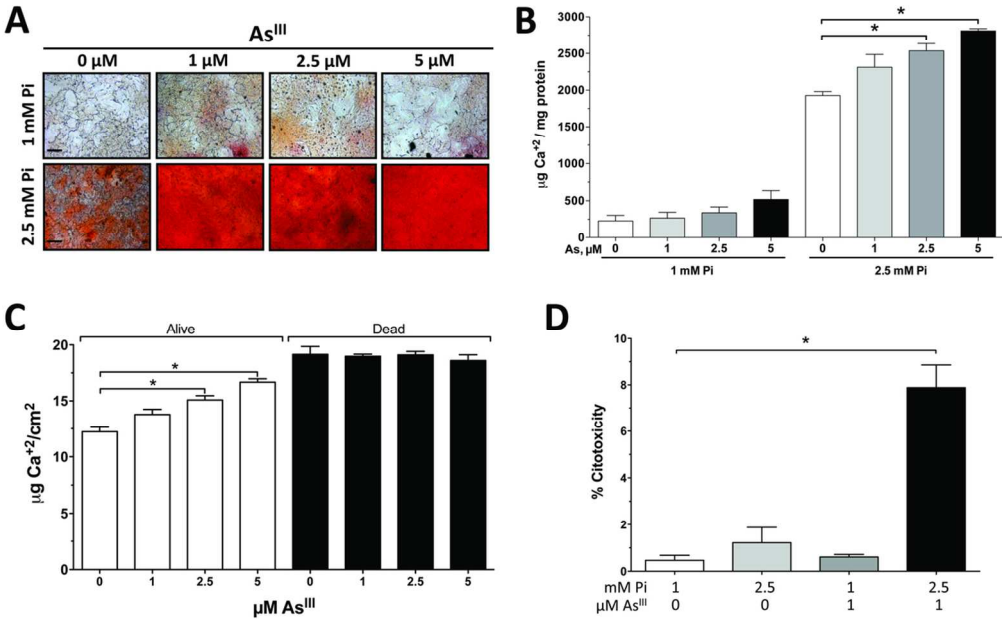

111x75mm (300 x 300 DPI)

Figure 3

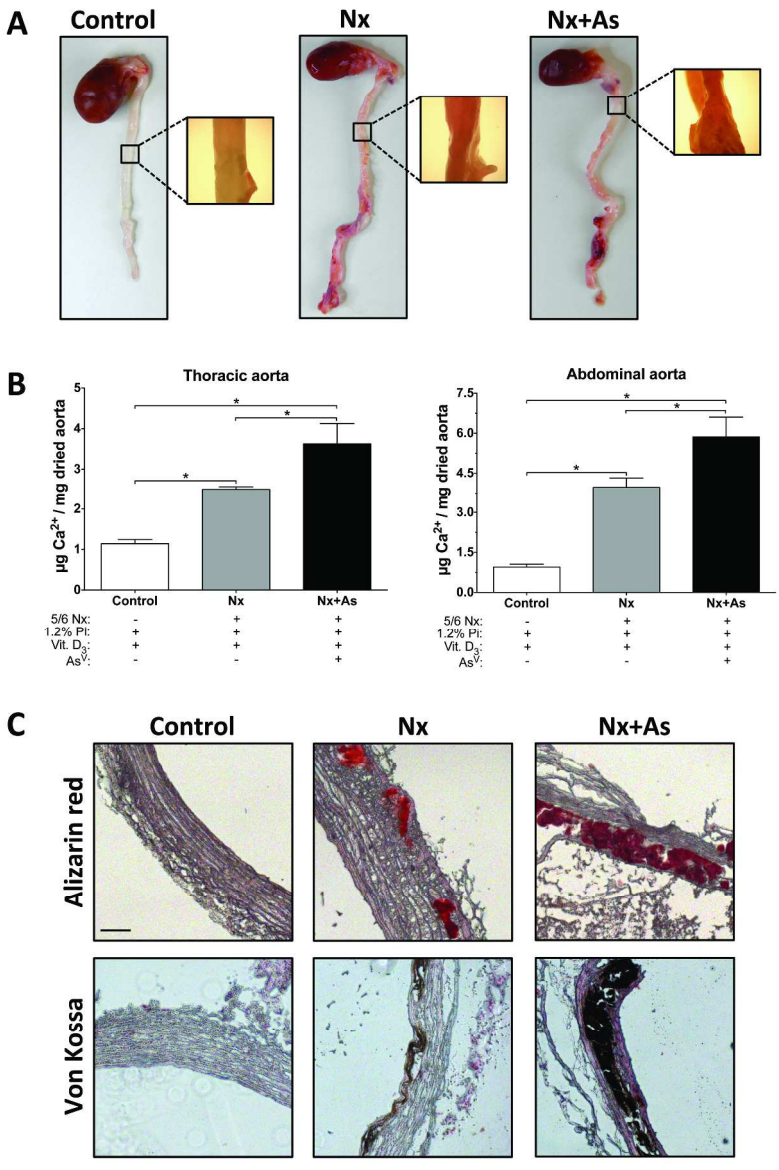

282x436mm (300 x 300 DPI)

Figure 4

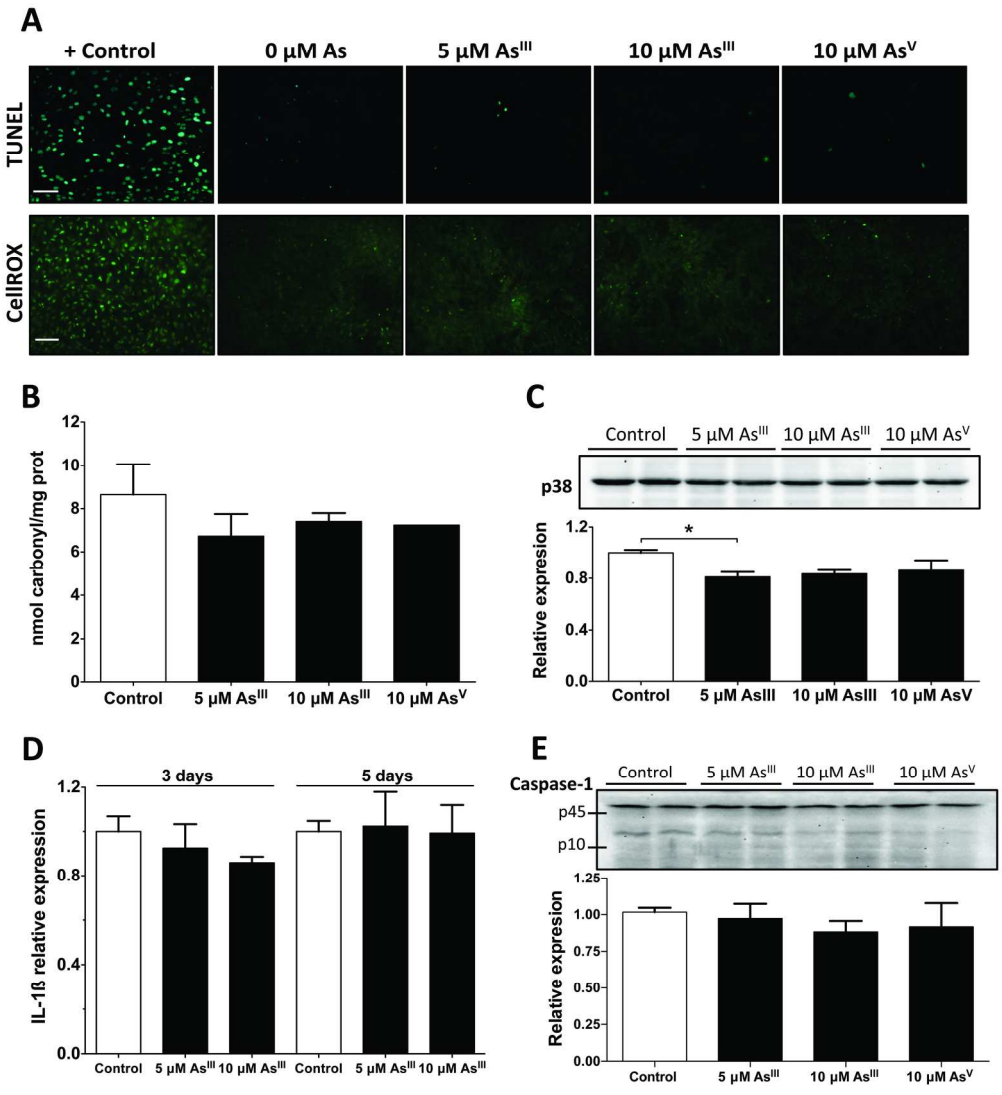

196x223mm (300 x 300 DPI)

Figure 5

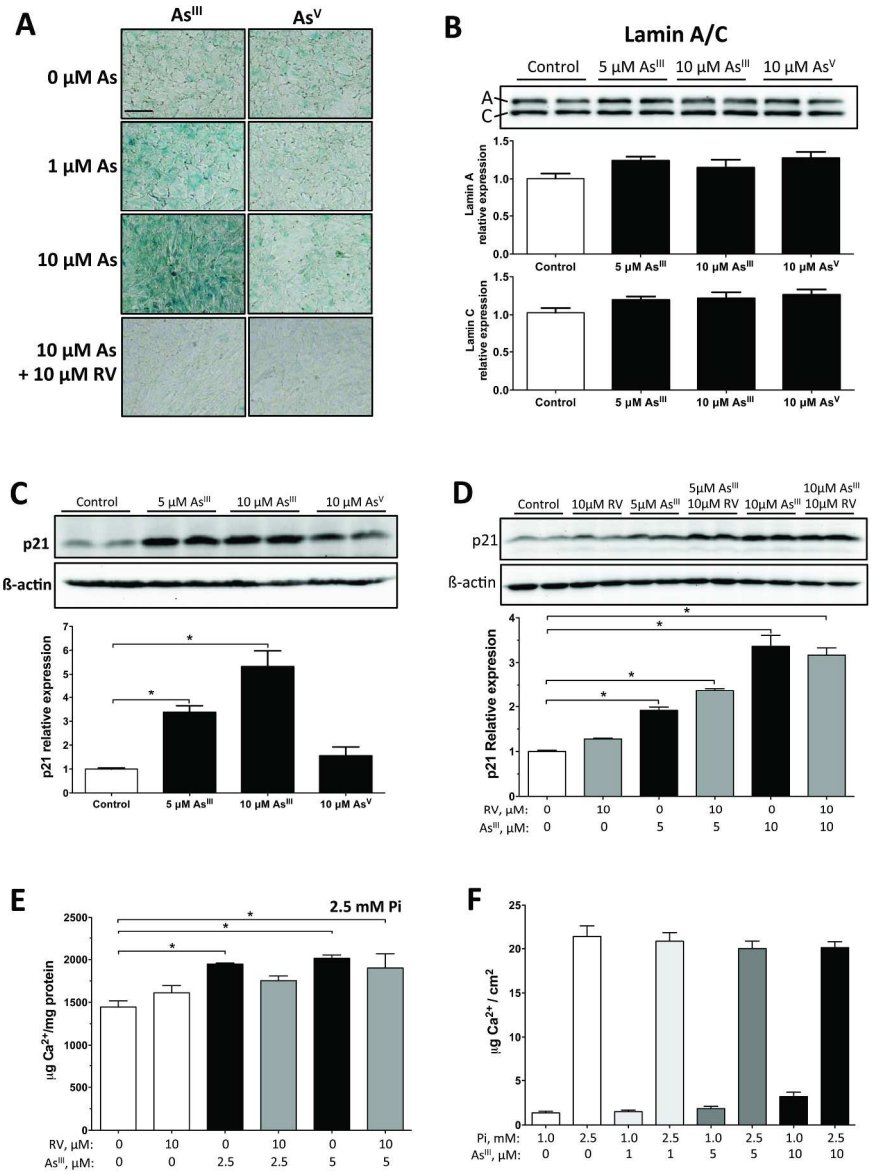

241x330mm (300 x 300 DPI)

Figure 6

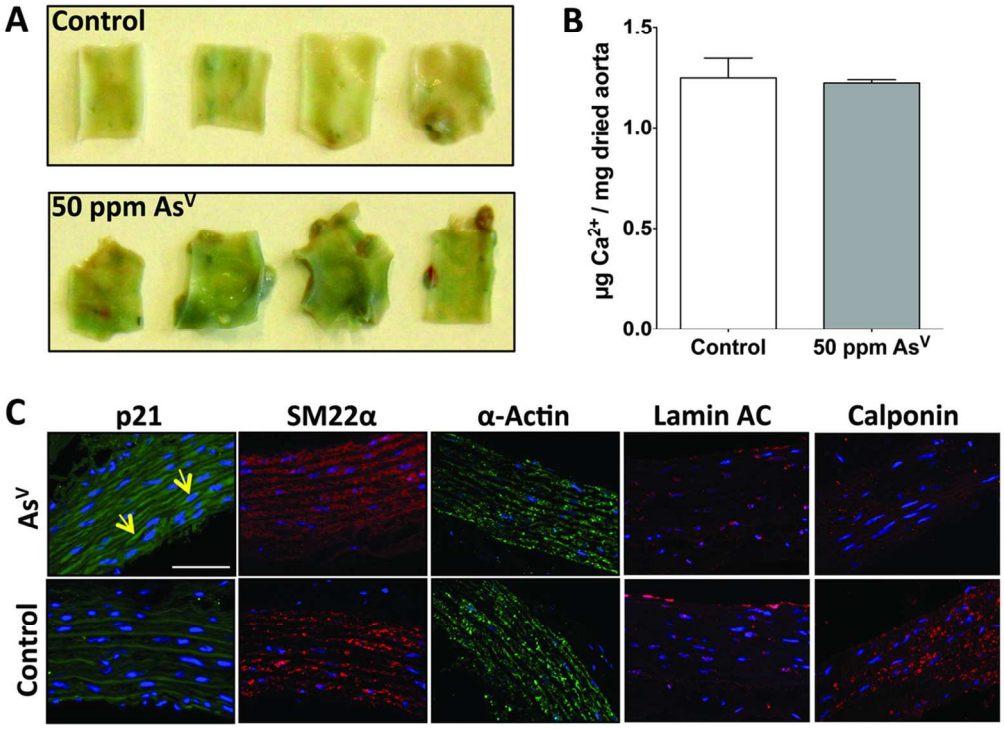

105x83mm (300 x 300 DPI)

Figure 7

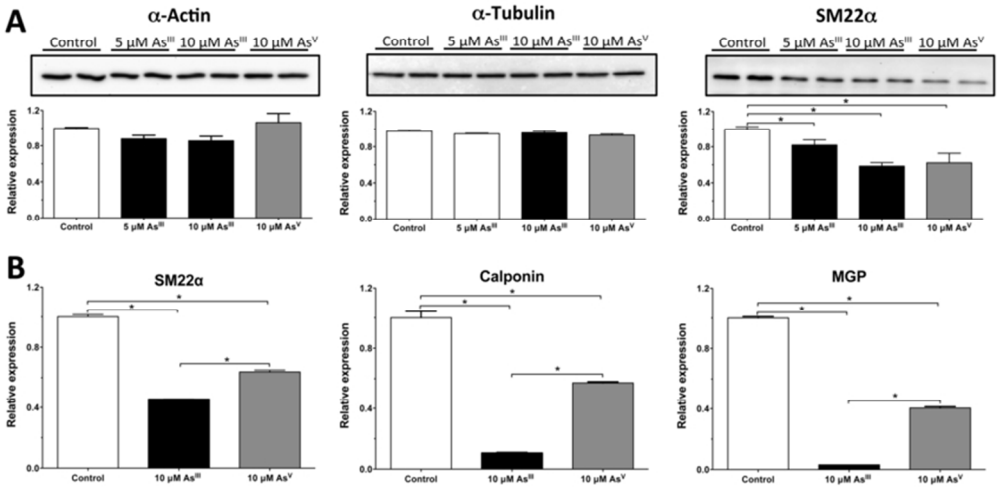

71x38mm (300 x 300 DPI)

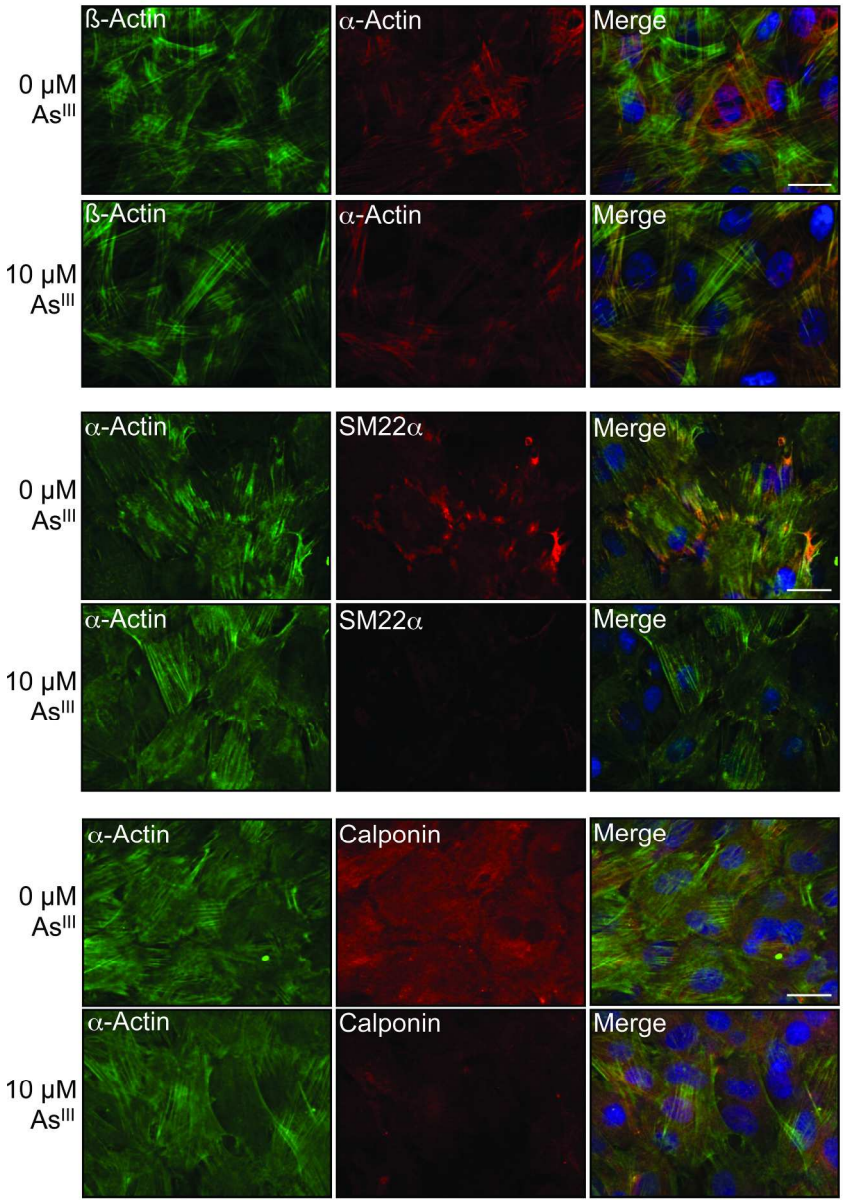

191x275mm (300 x 300 DPI)